CHAPTER 9

KINETICS AND MECHANISMS OF CHEMICAL REACTIONS IN CLOUDS AND FOGS

by

Michael R. Hoffmann

Environmental Engineering Science
W. M. Keck Laboratories
California Institute of Technology
Pasadena, California 91125

A paper presented at the

European Science Foundation Symposium on Cloud Chemistry

July, 1987
Cambridge, England

Introduction

Clouds, fogs, and haze aerosols are subjected to the same chemical processes because of their physical similarities. For example, cloud– and fogwater droplets are found in the size range of 2 to 50 μm, while deliquescent haze aerosol will be in the range of 0.01 to 1 μm. On the other hand, raindrops are approximately 100 times larger than cloud and fog water droplets (0.1 to 3 mm). However, a more important determinant of aqueous–phase chemistry within the droplets is the liquid water content (LWC); values of LWC range from 0.1 to 1.0 g m^{-3} in clouds, from 0.01 to 0.5 g m^{-3} in fogs, and from 10 to 100 μg m^{-3} in haze aerosols. The presence of condensation nuclei, which are composed of both soluble and insoluble materials, is essential for the formation of atmospheric water droplets. Accretion or evaporation of water to or from the condensation nuclei or droplet is forced by the difference between the ambient and local humidities, and is affected by the droplet surface tension and the chemical potential of the solutes in the liquid phase. During droplet growth, the temperature within the droplet differs from the ambient temperature due to the release of latent heat, which in turn depends upon the instantaneous growth rate.

Fog and cloud droplets are highly effective at scavenging certain gases and particles present in the atmosphere. The overall fraction of material incorporated into fog droplets depends upon nucleation scavenging and gas transfer. The initial chemical speciation may be altered by *in situ* chemical transformations and subsequent droplet–phase scavenging. The total concentration of species i in a parcel of air is given by

$$[C_i]_T = [C_i]L + P_{C_i}(RT)^{-1} + [C_i]_a \qquad (1)$$

where $[C_i]_T$ is the total concentration of C_i (mol m^{-3}) in the atmosphere, $[C_i]_f$ is the concentration of C_i in the droplet phase in units of mol m^{-3} ($[C_i]_f = L[C_i]$), $[C_i]_g$ is the concentration (mol m^{-3}) of C_i in the gas phase ($[C_i]_g = P_{C_i}(RT)^{-1}$), and $[C_i]_a$ is the

concentration of C_i in the non–activated aerosol. R is the universal gas constant (atm m^3 mol^{-1} K^{-1}) and T is temperature in degrees K.

Fog– and cloudwater often have extremely low pH values (e.g. $1.7 < pH < 4$) and extremely high concentrations of sulfate (1 to 20 mM), nitrate (1 to 20 mM, ammonium ion (0.1 to 20 mM) and trace metals (1 to 1000 μM). Waldman et al. (1) and Munger et al. (2) have summarized concentrations reported for fogs and clouds sampled in California and elsewhere around the world. Of special interest are the high values observed for SO_4^{2-}, NO_3^-, S(IV), CH_2O, Fe, Mn, Pb and Cu in fogwater. These values and their time–dependent changes indicate that fogs and clouds provide a very reactive environment for the accumulation of HNO_3 and H_2SO_4. Concomitant incorporation of NH_3 gas and calcareous dust into the droplet phase neutralizes some of the acidity. In the pH domain typically encountered in fogs and clouds (pH 2–7), absorption of $SO_2(g)$, $HNO_3(g)$, $H_2O_2(g)$, and $NH_3(g)$ is thermodynamically favorable because of their relatively high Henry's Law coefficients.

Of the metals commonly found in atmospheric water droplets, Fe, Mn and Cu are expected to be potential catalysts for the *in situ* oxidation of S(IV) with molecular oxygen. Iron and Mn have been found in concentrations as high as 400 μM and 15 μM in fog (1–7). Model calculations indicate that metal–catalyzed autoxidations along with oxidation by H_2O_2, O_3, and OH may contribute significantly to the overall sulfate formation rate in atmospheric droplets, particularly in the range of Fe and Mn concentrations observed in urban fog (8–10).

In addition to transition metal ions a wide variety of other chemical constituents have been found in clouds. For example, carbonyl compounds, such as aldehydes and ketones, have been found to influence liquid–phase sulfur dioxide chemistry through their reactions with SO_2 to form stable α–hydroxyalkanesulfonates. Field measurements have detected formaldehyde at concentrations of greater than 100 μM in fog– and cloudwater samples collected in Southern California (11–13). The concentrations of acetaldehyde.

glyoxal, methylglyoxal, and hydroxyacetaldehyde occasionally approach or exceed that of CH_2O. In addition to each one of the aldehydes present the corresponding carboxylic acid has been observed, although formic and acetic acid dominate the low molecular weight carboxylic acids. They are found found in concentrations as high as 100 μM.

The presence of CH_2O and H_2O_2 ($2 - 50$ μM)in conjunction with S(IV) at levels higher than those predicted by gas/liquid solubility equilibria suggests that α–hydroxymethanesulfonate (HMS, $HOCH_2SO_3^-$) production stabilizes a fraction of S(IV) with respect to oxidation. Equilibrium calculations using available thermodynamic and kinetic data for the reaction of SO_2 and CH_20 demonstrate that elevated concentrations of S(IV) in fog water cannot be achieved without consideration of sulfonic acid production, $HORHSO_3^-$ (11). Munger et al. (13) have identified and quantified HMSA using ion–pairing chromatography. Other S(IV) adducts which have been observed in cloudwater droplets include those formed with glyoxal, methylglyoxal, acetaldehyde, and hydroxyacetaldehyde.

Jacob et al. (14–17) have systematically characterized the interaction of H_2SO_4, HNO_3, NH_3 and in fog, aerosol, and the gas phase. The observed spatial patterns of concentrations were shown to closely reflect the distribution of SO_2, NO_x, and NH_3 emissions within well–defined regions. Furthermore, they (16) have compared field data for the H_2SO_4–HNO_3–NH_3 system with thermodynamic calculations of the aerosol composition. Close agreement has been found between field measurements and theoretical predictions. Their field studies have shown that typical wintertime conversion rates for S(IV) in fogs were about 5 % hr^{-2} and about 1 % hr^{-2} in haze aerosol.

Kinetic Considerations of Droplet–Phase Reactions

Gas–phase reactions of SO_2 with ozone (O_3), hydroxyl radical ($OH\cdot$), and hydroperoxyl radical ($HO_2\cdot$) are too slow to account for observed rates of sulfate production

in humid urban atmospheres (18–19) and in wave clouds (20). Consequently, the catalytic autoxidation of SO_2 in deliquescent haze aerosol and hydrometeors appears to be a viable non–photolytic pathway for the rapid formation of sulfuric acid in humid atmospheres (21–26). In addition, hydrogen peroxide and ozone have been established as important aqueous–phase oxidants of dissolved SO_2 (26). Oxidation by H_2O_2 seems to be most favorable under low pH conditions (pH $<$ 4) because of a rapid rate of reaction and a negative pH–dependence that favors the facile conversion of HSO_3^- to sulfate. In comparison, metal–catalyzed autoxidation and oxidation of S(IV) with O_3 tend to proceed more slowly with decreasing pH (27).

Limiting factors in the autoxidation pathways are the total concentration of the active metal catalyst and its equilibrium speciation as a function of pH. Los Angeles fog water contains high concentrations of iron, manganese, copper, nickel and lead (3,4,6,7). Of these metals, Fe, Mn and Cu are expected to be the most effective catalysts for the reaction of S(IV) with molecular oxygen (25–27). Model calculations indicate that metal–catalyzed autoxidations may contribute significantly to the overall sulfate formation rate in atmospheric droplets, particularly in the range of Fe and Mn concentrations observed in urban fog. However, the composition of the precursor haze aerosol or cloud condensation nuclei will determine to a large extent the observed chemical speciation of the droplet phase.

Chameides (28) has predicted based on model calculations that aqueous–phase free radical pathways can contribute substantially to the generation of acidity via the *in situ* oxidation of S(IV) and HCHO to S(VI) and formic acid, respectively. The principal oxidants of S(IV) as identified by Chameides were H_2O_2, O_3, $\cdot OH$, and $HO_2\cdot$. Parameters found to affect the S(IV) to S(VI) conversion rate were the accommodation coefficient for the reactive species of interest, the liquid water content, and the ambient levels of SO_2 and HNO_3. Seigneur and Saxena (29) have predicted that gas–phase hydrocarbon chemistry will dominate $\cdot OH$ chemistry (i.e., aqueous–phase $\cdot OH$ chemistry due to radical scavenging

appears to be inconsequential). While Mozurkewich (30) argues that nitrate radical, NO_3, is unlikely to play an important role in the nighttime chemistry of a cloud because of its low Henry's Law constant (~ 0.03 M atm^{-2}). Jacob (31) has shown that radical pathways are very important for the chemistry of remote clouds in terms of formate production and in terms of the buildup of peroxymonosulfuric acid, a S(VI)–peroxide intermediate of high oxidation potential.

Aqueous–phase pathways for the production of nitric acid are relatively minor contributors to nitrate accumulation in the droplet phase because of the low Henry's Law constants for NO_2 and NO and because of second–order reaction kinetics with respect to $[NO_2]$ (32–33). The predominant pathways for S(IV) transformation involve reactions with H_20_2, O_3, 0_2 (Fe^{3+} and Mn^{2+} catalyzed), $\cdot OH$, HONO, CH_3OOH, CH_3CO_3H, PAN, $HO_2\cdot$, HCHO, and soot.

A summary of rate expressions and kinetic data for these reactions is given in Table 1. In order to understand the potential importance of each reaction over a broad range of pH, a comparison of calculated reaction rates for an idealized cloud with a liquid water content (LWC) of 0.2 g m^{-3} at 25 ^0C and gas–phase concentrations of reactive components typical of the Los Angeles atmosphere can be made. We clearly see in these calculations that pH is the master variable for this comparative system of reactions. The simple calculations show that H_2O_2 is the most effective oxidant of S(IV) in an open–phase system over the entire pH range. Below pH 4.0, hydrogen peroxide appears to be the sole reactant capable of producing environmentally significant S(IV) oxidation rates. Above pH 4, a number of kinetic pathways in addition to the S(IV)–H_2O_2 reaction become viable potential contributors to net S(IV) oxidation. Ozone, $\cdot OH$, $HO_2\cdot$, HONO and Fe(III)– and Mn(II)–catalyzed autoxidation are major contributors to S(IV) oxidation above pH 4. With an idealized "sticking coefficient" of 1.0 for $\cdot OH$, the $\cdot OH$ pathway may proceed as rapidly as 500 % hr^{-1} at pH 5.0. Likewise, the predicted conversion rate for the above reactants at pH 5.0 are as follows: H_2O_2 (331 % hr^{-1}), O_3 (131 % hr^{-1}), $HO_2\cdot$ (2.0 % hr^{-1}), HONO (36.3

% hr^{-1}), $Fe(III)/O_2$ (200.0 % hr^{-1}), and $Mn(II)/O_2$ (95.5 % hr^{-1}). At slightly higher pH. PAN and peroxyacetic acid will contribute somewhat to the net S(VI) production rate.

In addition to the oxidation pathways for S(IV) mentioned above, one additional pathway for S(IV) transformation involves the reversible formation of α–hydroxymethane–sulfonate or other hydroxyalkylsulfonates or disulfonatess from the *in situ* reactions between RCHO and S(IV). The details of the thermodynamics of this system have been presented by Munger et al. (11) and Munger et al. (13). Using the kinetic data and rate law of Boyce and Hoffmann (34) as shown in Table 1 the calculated formation rate of $HOCH_2SO_3^-$ at pH 5.0 is 43.6 % hr^{-1} and at pH 7.0 it is 1.95 x 10^5 % hr^{-1}. These results suggest that RCHO/S(IV) adducts form preferentially near sources of SO_2 and RCHO in near–neutral, aquated haze aerosol. Because of the extremely slow dissociation kinetics for these adducts, the sulfonate complexes are metastable in more acidic environments with lower P_{SO_2} and P_{RCHO}. Unfavorable reaction kinetics at pH 3 does not necessarily mean that these adducts should not be found. It does indicate that proximity to sources and transport considerations are very important.

Reaction Mechanisms

Hydrogen Peroxide and Sulfur Dioxide

$$H_2O_2 + H_2O \cdot SO_2 \longrightarrow H_2O + H_2SO_4 \qquad (2)$$

The oxidation of aquated sulfur dioxide proceeds via a nucleophilic displacement of HSO_3^- by H_2O_2 to form peroxymonosulfurous acid as an intermediate which in turn undegoes an acid–catalyzed (both specific acid and general acid) rearrangement to give the products as described by the stoichiometry of equation 2 (36). The mechanism can be written as follows:

$$H_2O \cdot SO_2 \overset{K_{a1}}{\rightleftharpoons} H^+ + HSO_3^- \qquad (3)$$

$$HSO_3^- + H_2O_2 \underset{k_{-1}}{\overset{k_1}{\rightleftharpoons}} \underset{\substack{peroxymonosulfurous\\ acid}}{\overset{-O}{\underset{O}{\overset{\diagup}{\underset{\diagdown}{S}}}}\!\!=\!\!O\!-\!OOH} + H_2O \qquad (4)$$

$$\overset{-O}{\underset{O}{\overset{\diagup}{\underset{\diagdown}{S}}}}\!\!=\!\!O\!-\!OOH + H^+ \xrightarrow{k_2} H_2SO_4 \qquad (5)$$

$$\overset{-O}{\underset{O}{\overset{\diagup}{\underset{\diagdown}{S}}}}\!\!=\!\!O\!-\!OOH + HA \xrightarrow{k_3} H_2SO_4 + A^- \qquad (4)$$

This mechanism was originally proposed by Hoffmann and Edwards (37) and reaffirmed by many other investigators (38). Similar mechanisms have been proposed by Lind et al. (39) for the oxidation of S(IV) by methyl hydroperoxide, and peroxyacetic acid. The theoretical rate expression that results from this mechanism is as follows:

$$\nu = \frac{d[S(VI)]}{dt} = \frac{k_1 K_{a1}[H_2O_2]\,[\,S(IV)\,]}{(k_{-1} + k_2[H^+] + k_3[HA])\,(K_{a1} + [H^+])}(k_2[H^+] + k_3[HA]) \qquad (5)$$

where HA represents any general acid (i.e. weak acid or proton donor). This rate law reduces to the form given in Table 2 when the general acid–catalyzed pathway of eqn. 4 is ignored.

Ozone and Sulfur Dioxide

The oxidation of aquated sulfur dioxide by ozone (40)

$$H_nSO_3^{(n-2)} + O_3 \longrightarrow n\,H^+ + SO_4^{2-} + O_2 \qquad (5)$$

proceeds via three independent pathways that involve a nucleophilic attack on ozone by SO_3^{2-}, HSO_3^-, and $H_2O \cdot SO_2$. The starred oxygens indicate labeled oxygen (^{18}O).

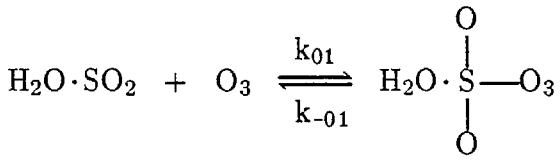

(6)

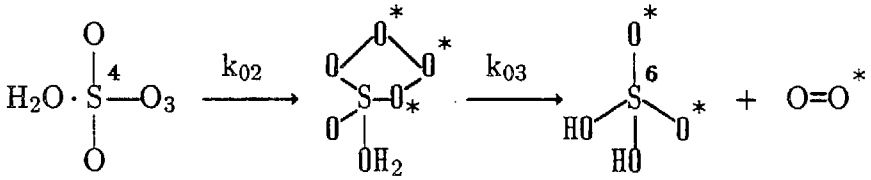

(7)

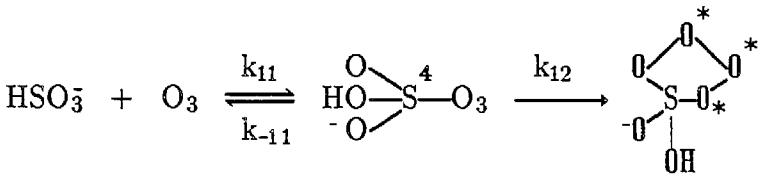

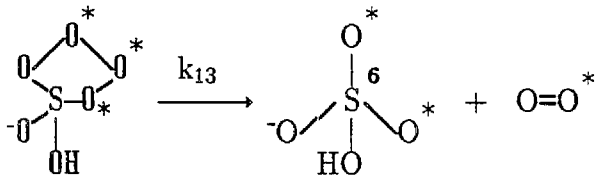

(8)

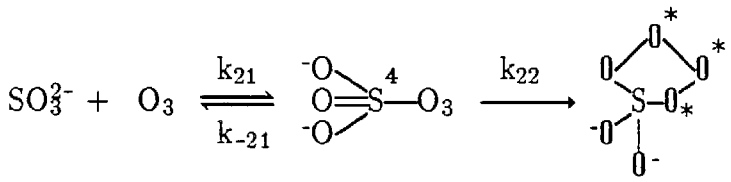

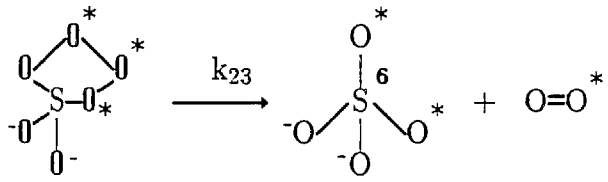

(9)

The theoretical rate expression that results from the mechanisms of eqns. 6–9 is as follows:

$$\nu = \left[\frac{k_{02}k_{01}}{(k_{-01} + k_{02})}[H_2O \cdot SO_2] + \frac{k_{12}k_{11}}{(k_{-11} + k_{12})}[HSO_3^-] + \frac{k_{22}k_{21}}{(k_{-21} + k_{22})}[SO_3^{2-}] \right][O_3] \qquad (10)$$

Equation 10 is readily reduced to the form given in Table 1.

Oxygen and Sulfur Dioxide as Catalyzed by Fe(III)

In light of our present work and the work of others (41–46) the following mechanism is proposed for the autoxidation of of S(IV):

$$HSO_3^- \overset{K_{a2}}{\rightleftharpoons} SO_3^{2-} + H^+ \qquad (11)$$

$$Fe^{3+} + H_2O \overset{*K_b}{\rightleftharpoons} FeOH^{2+} + H^+ \qquad (12)$$

$$FeOH^{2+} + SO_3^{2-} \overset{K_4}{\rightleftharpoons} \underset{\text{red complex}}{HOFeOSO_2} \qquad (13)$$

$$\underset{\text{red complex}}{HOFe'''OS^{iv}O_2} \underset{k_{-1}}{\overset{k_1}{\rightleftharpoons}} \underset{\text{orange complex}}{HOFe''OS^{v}O_2} \qquad (14)$$

$$\underset{\text{orange complex}}{HOFe''OS^{v}O_2} + O_2 \underset{k_{-2}}{\overset{k_2}{\rightleftharpoons}} HOFe'''OS^{v}O_2 \qquad (15)$$

$$\mathrm{HO\overset{\displaystyle O=O^{-}}{\overset{|}{Fe}}'''OS^{v}O_2} \xrightarrow{k_3} \mathrm{HO\overset{\displaystyle O=O^{2-}}{\overset{|}{Fe}}'''OS^{vi}O_2} \xrightarrow{+2H^+} \mathrm{HOFe^{2+}} + SO_3 + H_2O_2 \qquad (16)$$

$$SO_3 + H_2O \longrightarrow 2H^+ + SO_4^{2-} \qquad (17)$$

$$H_2O_2 + HSO_3^- \longrightarrow H_2O + H^+ + SO_4^{2-} \qquad (18)$$

A rate expression can be derived from the above mechanism be applying the steady–state approximation around the intermediate, $\mathrm{HO\overset{\displaystyle O=O^{-}}{\overset{|}{Fe}}'''OS^{v}O_2}$, such that the rate of production of sulfate is given by

$$\frac{d[SO_4^{2-}]}{dt} = k_3\left[\mathrm{HO\overset{\displaystyle O=O^{-}}{\overset{|}{Fe}}'''OS^{v}O_2}\right] \qquad (19)$$

or

$$\frac{d[SO_4^{2-}]}{dt} = \left[\frac{k_2}{k_3 + k_{-2}}\right]\left[\frac{k_1}{k_2[O_2] + k_{-1}}\right] K_4\alpha_1\beta_1[Fe(III)][S(IV)][O_2] \qquad (20)$$

We can reduce Eq. 20 to the following form by assuming that $k_3 >> k_{-2}$ and $k_2[O_2] >> k_{-1}$ (these approximations are valid given the magnitude of stability constants (i.e. $K_2' = k_2/k_{-2}$) and rate constants for ligand substitution):

$$\frac{d[SO_4^{2-}]}{dt} = k_1K_4\alpha_2\beta_1[Fe(III)][S(IV)] \qquad (21)$$

At pH 4, $\beta_1 \sim 1$, $k_1 \sim 0.04\ s^{-1}$ and $k_1K_4 = 1.0 \times 10^6\ M^{-1}s^{-1}$. If we compare the predicted rate expression of Eq. 21 to the composite rate law (Eq. 22) obtained by analysis of the empirical data given the investigators listed in Table 3,

$$-\frac{d[S(IV)]}{dt} = k[Fe(III)][S(IV)]\alpha_2 \qquad (22)$$

we see that $k \simeq k_1K_4$. The value obtained for k given in Table 4 is $1.2 \times 10^6\ M^{-1}s^{-1}$ while the calculated value of k_1K_4 is $1.0 \times 10^6\ M^{-1}s^{-1}$ (41). The active catalytic intermediate of Eq. 19 can be drawn as follows:

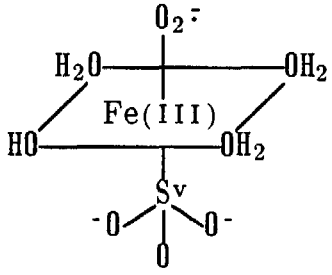

in order to reflect the known geometry for octahedrally–coordinated Fe(III) and to reflect the Fe–O–S mode of bonding as determined by Raman measurements (41).

Although Fe has been found in high ($\simeq$ 100 μM) concentrations in atmospheric droplets, much of this iron would be in form of solid particles or colloids. Ferric oxides, such as Fe_2O_3, have been identified as components of airborne particles. Other sulfite complexes, such as α–hydroxyalkylsulfonates, have larger stability constants than the Fe(III)–S(IV) complexes (K for the HSO_3^-/HCHO adduct = $[HOCH_2SO_3^-]/[HCHO]_T[HSO_3^-]$, = 10^7. Thus, given the stability constant $K_1 = 10^{6.6}$ for $FeSO_3^+$, the ratio of $[Fe(III)]_T$:$[HCHO]_T$ would have to be approximately 30 at pH 2 or 3×10^2 at pH 5 for comparable concentrations of $FeSO_3^+$ to coexist with $HOCHSO_3^-$. Aldehydes have been found in much higher concentrations than Fe(III) in cloud–, fog– and rainwater systems.

therefore S(IV) speciation is likely to be dominated by $RC(OH)SO_3^-$ chemistry rather than $Fe(SO_3)_n^{3-2n}$.

Formation of Carbonyl–S(IV) Adducts

The reversible formation of S(IV)–carbonyl adducts occurs via nucleophilic addition. This involves the attack of a nucleophile, with its lone–pair electrons, on the carbon atom of the carbonyl group. Using sulfite as an example, the addition step and associated displacement of electrons can be illustrated as follows:

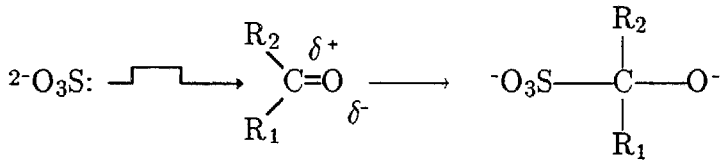

Polarization induced by the electronegative carbonyl oxygen and by the substituents R_1 and R_2 results in a partial positive charge at the carbon atom and hence a favorable site for nucleophilic attack. As sulfite approaches the carbon atom, oriented perpendicular to the plane of the carbonyl group, it displaces a pair of π–bond electrons and forms a stable σ–bond.

The order of increasing reactivity among aqueous S(IV) species has been experimentally demonstrated to be in the direction of increasing nucleophilic character (47–53): $H_2O \cdot SO_2 < HSO_3^- < SO_3^{2-}$. The second–order rate constants for the reaction of bisulfite and sulfite with isobutyraldehyde, formaldehyde, benzaldehyde, and methylglyoxal are compared in Table 4. The transition state for reaction with HSO_3^- may involve a cyclic, high entropy intermediate whereas that for SO_3^{2-} does not; and that the difference in entropy of activation is a major reason for the faster addition reactions of SO_3^{2-}.

The following elementary steps adequately describe the reaction of most aldehydes

with S(IV).

$$RCH(OH)_2 \overset{K_d}{\rightleftharpoons} RCHO + H_2O \tag{23}$$

$$H_2O \cdot SO_2 \overset{K_{a1}}{\rightleftharpoons} H^+ + HSO_3^- \tag{24}$$

$$HSO_3^- \overset{K_{a2}}{\rightleftharpoons} H^+ + SO_3^{2-} \tag{25}$$

$$HSO_3^- + RCHO \underset{k_{-1}}{\overset{k_1}{\rightleftharpoons}} RCH(OH)SO_3^- \tag{26}$$

$$SO_3^{2-} + RCHO \underset{k_{-2}}{\overset{k_2}{\rightleftharpoons}} RCH(O^-)SO_3^- \tag{27}$$

$$RCH(OH)SO_3^- \overset{K_{a3}}{\rightleftharpoons} RCH(O^-)SO_3^- + H^+ \tag{28}$$

$$RCHO + H^+ \overset{K_H}{\rightleftharpoons} RCHOH^+ \tag{29}$$

$$RCHOH^+ + HSO_3^- \underset{k_{-3}}{\overset{k_3}{\rightleftharpoons}} RCH(OH)SO_3^- + H^+ \tag{30}$$

The theoretical rate expression that results from this mechanism has the following form far from equilibrium:

$$\frac{d[RCH(OH)SO_3^-]}{dt} = (k_1[SO_3^{2-}] + k_2[HSO_3^-] + k_3K_H[H^+][HSO_3^-])[RCHO] \tag{31}$$

Heterogeneous Photocatalytic Oxidation of Sulfur Dioxide

Metal oxide semiconductors such as α–Fe_2O_3 can function either as photosensitizers or as photocatalysts (54). Absorption of a photon with an energy equal to or greater than the bandgap energy, E_g, of a semiconductor results in the transient formation of an electron/hole pair (i.e. exciton).

$$\alpha\text{–}Fe_2O_3 \xrightarrow{h\nu} e^-_{cb} + h^+_{vb} \tag{32}$$

In the absence of suitable electron and hole scavengers adsorbed to the surface of a semiconductor particle, recombination occurs within 100 ns. However, when appropriate scavengers are present the valance band holes, h^+_{vb}, function as powerful oxidants while the conduction band electrons, e^+_{cb}, function as moderately powerful reductants. Aquated sulfur dioxide can be readily oxidized on the particle surface as follows:

$$h^+_{vb} + SO_3^{2-} \longrightarrow SO_3^{-}\cdot \tag{33}$$

$$SO_3^{-}\cdot + O_2 \longrightarrow SO_3 + O_2^{-}\cdot \tag{34}$$

$$SO_3 + H_2O \longrightarrow SO_4^{2-} + 2\,H^+ \tag{35}$$

$$O_2^{-}\cdot + H^+ \rightleftharpoons HO_2\cdot \tag{36}$$

$$O_2^{-}\cdot + HO_2\cdot + H^+ \longrightarrow H_2O_2 + O_2 \tag{37}$$

The rate law that arises from this surface–limited mechanism is

$$\nu = \Phi\beta(1 - e^{\gamma\{Fe_2O_3\}})\left[\frac{K[HSO_3^-]}{1 + K[HSO_3^-]}\right] \tag{38}$$

where Φ is the instrinsic quantum yield { i.e. S(IV) + $h^+_{cb} \longrightarrow SO_3^-\cdot$ }, K is the adsorption equilibrium constant, β is the incident photon flux (M min^{-1}), $\{Fe_2O_3\}$ is the mass concentration of catalyst (g L^{-1}), and γ is a function of the apparent absorptivity of the solid (L g^{-1}). When the number of reactive surface sites is limiting desorption of $SO_3^-\cdot$ radical from the surface can occur. This will lead to the following free radical chain reaction in aqueous solution:

$$SO_3^-\cdot + O_2 \xrightarrow{k_1} SO_5^-\cdot \tag{39}$$

$$SO_5^-\cdot + HSO_3^- \xrightarrow{k_2} SO_4^-\cdot + SO_4^{2-} + H^+ \tag{40}$$

$$SO_4^-\cdot + HSO_3^- \xrightarrow{k_3} SO_3^-\cdot + SO_4^{2-} + H^+ \tag{41}$$

$$2\ SO_3^-\cdot \xrightarrow{k_4} S_2O_6^{2-} \tag{42}$$

$$2\ SO_4^-\cdot \xrightarrow{k_5} S_2O_6^{2-} + O_2 \tag{43}$$

$$2\ SO_5^-\cdot \xrightarrow{k_6} S_2O_6^{2-} + 2\ O_2 \tag{44}$$

An additional free–radical termination step involves the surficial reaction of $SO_5^-\cdot$

$$\equiv| -SO_5^- \cdot \; + \; h^+_{vb} \xrightarrow{k_8} \equiv| -SO_3 \; + \; O_2 \qquad (45)$$

Given this mechanism the following rate expression is obtained (55):

$$-\frac{d[S(IV)]}{dt} = -\frac{k_3 k_8}{4k_7}\{M_xO_y\}[HSO_3^-] +$$

$$[HSO_3^-]\sqrt{\left[\frac{k_3k_8}{4k_7}\right]^2\{M_xO_y\}^2 + \frac{k_3^2}{2k_7}\Phi\beta(1 - e^{\gamma\{M_xO_y\}})\left[\frac{K[HSO_3^-]}{1 + K[HSO_3^-]}\right]} \qquad (46)$$

The photocatalytic production of hydrogen peroxide on particle surfaces has been clearly established (56).

$$O_2 \; + \; 2\, e^-_{cb} \; + \; 2\, H^+ \longrightarrow H_2O_2 \qquad (47)$$

In addition to the photocatalytic production of peroxide, the photocatalytic oxidation of weak organic acids such as acetate/acetic acid can proceed simultaneously as follows:

$$2\, CH_3COO^- \; + \; 2\, h^+_{vb} \xrightarrow[TiO_2]{h\nu} C_2H_6 \; + \; 2\, CO_2 \qquad (48)$$

$$HOOCCOOH \; + \; 2\, h^+_{vb} \xrightarrow[TiO_2]{h\nu} 2\, CO_2 \; + \; 2\, H^+ \qquad (49)$$

References

1. Liljestrand, H. M. Ph.D. Thesis, California Institute of Technology, Pasadena, 1980.

2. Liljestrand, H. M.; Morgan, J. J. *Environ. Sci. Technol.* 1981, **15**, 333–338.

3. Waldman, J. M.; Munger, J. W.; Jacob, D. J.; Hoffmann, M. R. *Tellus* 1985, **37B**, 91–108.

4. Munger, J. W.; Jacob, D. J.; Waldman, J. W.; Hoffmann, M. R. *J. Geophys. Res.* 1983, **88C**, 5109–5121.

5. Jacob, D. J.; Wang, R. T.; Flagan, R. C. *Environ. Sci. Tech.* 1984, **18**, 827–833.

6. Jacob, D. J.; Waldman, J. M.; Munger, J. W.; Hoffmann, M. R. *Environ. Sci. Technol.* 1985, **19**, 730–735.

7. Waldman, J. M.; Munger, J. W.; Jacob, D. J.; Flagan, R. C.; Morgan, J. J.; Hoffmann, M. R. *Science,* **218**, 677–680.

8. Jacob, D. J.; Hoffmann, M. R. *J. Geophys. Res.* 1983, 88, 6611–6621.

9. Jacob, D. J. Ph.D. Thesis, California Institute of Technology, Pasadena, 1985.

10. Hoffmann, M. R.; Jacob, D. J.; in "SO_2, NO and NO_2 Oxidation Mechanisms: Atmospheric Consideration"; Calvert, J. G., Ed.; ACID PRECIPITATION SERIES Vol. 3, Butterworth Publishers: Boston, 1984; 101–172.

11. Munger, J. W., Jacob, D. J., and Hoffmann, M. R., *J. Atmos. Chem.* 1984, 1, 335–350.

12. Waldman, J. M. Ph.D. Thesis, California Institute of Technology, Pasadena, CA, 1986.

13. Munger, J. W.; Tiller, C.; Hoffmann, M. R. *Science* 1986, **231**, 247–249.

14. Jacob, D. J.; Waldman, J. M.; Munger, J. W.; Hoffmann, M. R. *Tellus* 1984, **36B**, 272–285.

15. Jacob, D. J.; Waldman, J. M.; Munger, J. W.; Hoffmann, M. R. *J. Geophys Res.* 1986, **91D**, 1089–1096.

16. Jacob, D. J.; Munger, J. W.; Waldman, J. M.; Hoffmann, M. R. *J. Geophys Res.* 1986, **91D**, 1073–1088.

17. Jacob, D. J.; Shair, F. H.; Waldman, J. M.; Munger, J. W.; Hoffmann, M. R. *Atmos. Environ.* 1987, **21**, 1305–1313.

18. Calvert, J. G. in Acid Precipitation, SO_2, NO, and NO_2 Oxidation Mechanisms: Atmospheric Considerations, Butterworth Publishers, Stoneham, MA (1984).

19. Cass, G. R., Ph.D. Thesis, California Institute of Technology, Pasadena, CA (1977).

20. Hegg, D. A.; Hobbs, P. V. *Atmos. Environ.* 1982, **16**, 2663–2668.

21. Hegg, D. A. and Hobbs, P. V. *Atmos. Environ.* 1978, **12**, 241–253.

22. Kaplan, D. J., Himmelblau, D. M. and Kanaoka, C. *Atmos. Environ.* 1981, 15, 763–773.

23. Penkett, S. A., Jones, B. M. R. and Eggleton, A. E. J. *Atmos. Environ.* 1979, 13, 139–147.

24. Penkett, S. A., Jones, B. M. R., Brice, K. A. and Eggleton, A. E. J. *Atmos. Environ.* 1979, **13**, 123–137

25. Beilke, S. and Gravenhorst, G. *Atmos. Environ.* 1978, **12**, 231–239.

26. Martin, L. R. "Kinetic Studies of Sulfite Oxidation in Aqueous Solution," in Acid Precipitation, edited by J. G. Calvert, Butterworth Publishers, Stoneham, MA, 63–100 (1984).

27. Hoffmann, M. R. and Boyce, S. D. "Catalytic Autoxidation of Aqueous Sulfur Dioxide in Relationship to Atmospheric Systems," in Trace Atmospheric Constituents: Properties, Transformations and Fates, S. E. Schwartz, ed. Adv. *Environ. Sci. Technol.* 1983, **12**, 147–189.

28. a. Chameides, W. L. and D. D. Davis, *J. Geophys. Res.,* 1982, **87C**, 4863–4877.

    b. Chameides, W. L., *J. Geophys. Res.,* 1984, **89D**, 4739–4755.

    c. Chameides, W. L., *J. Geophys. Res.* 1986, **91D**, 5331–5337.

29. Seigneur, C. and P. Saxena, *Atmos. Environ.* 1984, **18**, 2109–2124.

30. Mozurkewich, M., *J. Geophys. Res.* 1986, **91D**, 14569–14570.

31. Jacob, D. J., *J. Geophys. Res.* 1986, **91D**, 9807–.

32. Lee, Y. N. and Schwartz, S. E., *J. Geophys. Res.,* 1981, **86**, 11971–11983.

33. Schwartz, S. E., "Gas–Aqueous Reactions of Sulfur and Nitrogen Oxides in Liquid–Water Clouds," in *SO_2, NO and NO_2 Oxidation Mechanisms: Atmospheric Considerations*, Calvert, J. G., Ed.; Butterworth: Boston, 1984; Vol. 3, pp. 173–208.

34. Boyce, S. D.; Hoffmann, M. R. *J. Phys. Chem.* 1984, **88**, 4740–4746.

35. Hoffmann, M. R. and Calvert, J. G. "Chemical Transformation Modules for Eulerian Acid Deposition Models Vol.II: The Aqueous–Phase Chemistry," EPA/NCAR Report DW 930237, March (1985).

36. J. V. McArdle and M. R. Hoffmann, 1983, *J. Phys. Chem.*, **87**, 5425–5429.

37. M. R. Hoffmann and J. O. Edwards, 1975, *J. Phys. Chem.*, **79**, 2096–2098.

38. a. Kunen, S. M., A. L. Lazrus, G. L. Kok, and G. G. Heikes, *J. Geophys. Res.* 1983, **88**, 3671–

b. Y. –N. Lee, J. Shen, P. J. Klotz, S. E. Schwartz, and L. Newman, *J. Geophys. Res.* 1986, **91D**, 13264–13274.

c. Martin, L. R. and D. E. Damschen, *Atmos. Environ.* 1981, **15**, 1615–

d. Overton, J. H., Jr., *Atmos. Environ.* 1985, **19**, 687–

39. J. A. Lind, A. L. Lazrus, and G. L. Kok, *J. Geophys. Res.* 1986, **92D**, 4171–4178.

40. Hoffmann, M. R. *Atmos. Environ.* 1986, **20**, 1145–1154.

41. a. Hoffmann, M. R. and A. P. K. Hong, *Sci. Total Environ.* 1987, **64**, 99–115.

b. Conklin, M. H. and M. R. Hoffmann, "Metal Ion–S(IV) Chemistry I., II.,& III., in press, *Environ. Sci. Technol.* 1988, **22**, 000–000.

42. Fuzzi, S., 1978, *Atmos. Env.*, **12**, 1439–1442.

43. Brimblecombe, P. and D.J. Spedding, 1974, *Atmos. Env.*, **8**, 937–945.

44. Neytzell–de Wilde, F.G. and L. Traverner in *2nd U.N. Intl. Conf. Peaceful Uses for Atomic Energy Proc. Vol. 3* (1958), pp. 303–317.

45. Aubuchon, C., *The Rate of Iron Catalyzed Oxidation of Sulfur Dioxide by Oxygen in Water* (Ph.D. Thesis, John Hopkins U., Baltimore, MD, 1976).

46. Olson, T.M., S.D. Boyce and M.R. Hoffmann, 1986, *J. Phys. Chem.*, **90**, 2482–2488.

47. Olson, T.M. and M.R. Hoffmann, 1986, *Atmos. Env.*, **20**, 2277–2278.

48. Skrabal, A. and R. Skrabal, 1936, *Sitz. Akad. Wirs. Wien*, **145**, 617–647.

49. Green, L. R. and J. Hine, 1974, *J. Org. Chem.*, **39**, 3896–3901.

50. Gubareva, M.A. *J. Gen. Chem. (USSR)* 1947, **17**, 2259–64.

51. Betterton, E.A., and M.R. Hoffmann, 1987, *J. Phys. Chem.* **91**, 3011–3020.

52. Betterton, E. A., Y. Erel and M. R. Hoffmann, 1988, *Environ. Sci. Technol.* 22, 92–99, 1987.

53. Olson, T. M. and M. R. Hoffmann, 1988, *J. Phys. Chem.* **92**, 533–540.

54. Bahnemann, D. W. and M. R. Hoffmann, 1987, *Proc. Electrochem. Soc.*, "Stabilization of Free Radical Intermediates on Metal Oxide Surfaces."

55. Hong, A., D. W. Bahnemann, and M. R. Hoffmann, 1987, *J. Phys. Chem.* 91, 6245–6251.

54. Kormann, C., D. Bahnemann, and M. R. Hoffmann, 1988, *Environ. Sci. Technol.*, 22, 000–000.

Table 1. Recommended Rate Laws and Rate Constants According to Hoffmann and Calvert (35) for 25.0 °C for the Oxidation of S(IV) in Aqueous Solution.

$$\nu \equiv -d[S(IV)]/dt$$

OXIDANT	RATE LAW & RATE CONSTANTS
O_3	$\nu = (k_0\alpha_0 + k_1\alpha_1 + k_2\alpha_2)[O_3][S(IV)]$ $k_0 = 2.40 \times 10^4$ $(M^{-1}s^{-1})$ $k_1 = 3.70 \times 10^5$ $(M^{-1}s^{-1})$ $k_2 = 1.50 \times 10^9$ $(M^{-1}s^{-1})$
H_2O_2	$\nu = k[H^+][H_2O_2][S(IV)]\alpha_1(1 + K[H^+])^{-1}$ $k = 7.50 \times 10^7$ $(M^{-2}s^{-1})$ $K = 13$ M^{-1}
$\cdot OH$	$\nu = (k_1\alpha_1 + k_2\alpha_2)[OH][S(IV)]$ $k_1 = 9.50 \times 10^9$ $(M^{-1}s^{-1})$ $k_2 = 5.50 \times 10^9$ $(M^{-1}s^{-1})$
HONO	$\nu = k[H^+][HSO_3^-][NO_2^-]$ $k = 1.75 \times 10^7$ $(M^{-1}s^{-1})$
CH_3OOH	$\nu = k[H^+][CH_3OOH][S(IV)]\alpha_1$ $k = 1.75 \times 10^7$ $(M^{-1}s^{-1})$
CH_3CO_3H	$\nu = (k_3[H^+] + k_2)[HSO_3^-][CH_3CO_3H]$ $k_3 = 3.64 \times 10^7$ $(M^{-1}s^{-1})$ $k_2 = 6.01 \times 10^2$ $(M^{-1}s^{-1})$
PAN	$\nu = k[PAN][S(IV)]\alpha_2$ $k = 1.0 \times 10^5$ $(M^{-1}s^{-1})$
$Fe(III)/O_2$	$\nu = k[Fe(III)][S(IV)]\alpha_2$ $k = 1.20 \times 10^6$ $(M^{-1}s^{-1})$
Mn/O_2	$\nu = k_2[Mn(II)][S(IV)]\alpha_1 + k_1K_1[Mn(II)]^2$ $k_2 = 3.40 \times 10^3$ $(M^{-1}s^{-1})$ $k_1 = 2.0 \times 10^9$ $(M^{-1}s^{-1})$ $K_1 = 1.26 \times 10^{-10}$

Soot	$\nu = k_1 K_1 [C_x][S(IV)]^2 A^{-1}$
	$A = 1 + K_2[S(IV)] + K_1[S(IV)]^2$
	$k_1 = 1.04 \times 10^7$ (mol $g^{-1}s^{-1}$)
	$K_1 = 4.92 \times 10^8$ (M^{-2})
	$K_2 = 2.96 \times 10^5$ (M^{-1})
HCHO	$\nu = (k_1\alpha_1 + k_2\alpha_2)K_d[S(IV)][HCHO]_T(K_d + 1)^{-1}$
	$k_1 = 79$ ($M^{-1}s^{-1}$)
	$k_2 = 2.48 \times 10^7$ ($M^{-1}s^{-1}$)
	$K_d = 5.5 \times 10^{-4}$
$HO_2\cdot$	$\nu = (k_1\alpha_1\beta_0 + k_2\alpha_2\beta_1)[S(IV)][HO_2]_T$
	$k_1 = 1.0 \times 10^6$ ($M^{-1}s^{-1}$)
	$k_2 = 1.0 \times 10^5$ ($M^{-1}s^{-1}$)
	$K_{a1} = 1.3 \times 10^{-5}$ (M^{-1})
	$\beta_0 = K_{a1}([H^+] + K_{a1})^{-1}$
	$\beta_1 = [H^+]([H^+] + K_{a1})^{-1}$

Table 2. Henry's Law Constants and Acidity Constants at 25.0 °C.

Species	[C] (atm)	H (M atm^{-1})	[C] (M)	pK_1	pK_2
HONO	1.0×10^{-9}	4.9×10^1	4.9×10^{-8}	3.15	———
CH_3OOH	2.0×10^{-11}	1.0×10^3	2.0×10^{-7}	11.5	———
CH_3COO_2H	1.0×10^{-12}	1.0×10^4	1.0×10^{-7}	8.20	———
PAN	3.0×10^{-8}	3.6×10^0	1.1×10^{-7}	———	———
HO_2	4.0×10^{-12}	5.0×10^4	2.0×10^{-6}	4.45	———
HCHO	3.0×10^{-8}	6.3×10^3	1.9×10^{-4}	———	———
OH	1.0×10^{-13}	2.0×10^2	2.0×10^{-22}	11.9	———
H_2O_2	1.0×10^{-9}	1.6×10^5	1.6×10^{-4}	11.65	———
O_3	5.0×10^{-8}	1.0×10^{-2}	5.0×10^{-11}	———	———
SO_2	2.0×10^{-8}	1.2×10^0	3.2×10^{-5}	1.89	7.22

$[S(IV)] = H_{SO_2} P_{SO_2} \alpha_0^{-1}$, $\alpha_0 \equiv [SO_2\cdot H_2O]/[S(IV)]$, $\alpha_1 \equiv [HSO_3^-]/[S(IV)]$, $\alpha_2 \equiv [SO_3^{2-}]/[S(IV)]$,
pH = 5.0

$$\alpha_0 = \frac{[H^+]^2}{([H^+]^2 + K_{a1}[H^+] + K_{a1}K_{a2})}$$

$$\alpha_1 = \frac{K_{a1}[H^+]}{([H^+]^2 + K_{a1}[H^+] + K_{a1}K_{a2})}, \quad \alpha_2 = \frac{K_{a1}K_{a2}}{([H^+]^2 + K_{a1}[H^+] + K_{a2}K_{a2})}$$

Table 3. Formation Constants for Selected Bisulfite–Aldehyde Adducts

Aldehyde	$^{e}K_1$*	K_1†	T(°C)	μ (M)	Ref.
HCHO	8.33×10^6	6.60×10^9	25	0.01	(48)
CH_3CHO	–	6.90×10^5	25	0.02	(52)
CH_3CH_2CHO	1.30×10^4	–	20	0.01	(49)
C_6H_5CHO	4.80×10^3	9.55×10^3	25	1.00	(47)
CHOCHO	2.81×10^4	–	25	0.02	(53)
CH_3COCHO	8.21×10^8	8.13×10^8	25	0.20	(51)
$HOCH_2CHO$	–	2.00×10^6	25	0.20	(52)

* $^{e}K_1 = [RCH(OH)SO_3^-]/([RCHO] + [RCH(OH)_2])[HSO_3^-]$ (M).
† $K_1 = [RCH(OH)SO_3^-]/[RCHO][HSO_3^-]$ (M).

Table 4. Rate Constants for the Rate Expression of Eqn. 31 (25 °C).

RCHO	k_2 ($M^{-1}s^{-1}$)	k_1 ($M^{-1}s^{-1}$)	μ (M)	Ref.
HCHO	2.48×10^7	7.90×10^2	1.0	(34)
C_6H_5CHO	2.10×10^4	0.71	1.0	(47)
$(CH_3)_2CHCHO$	1.40×10^4	–	0.1	(48)
CH_3COCHO	3.66×10^8	3.45×10^3	0.2	(51)
CHOCHO	1.04×10^7	6.50×10^2	0.2	(53)

METHYL HYDROPEROXIDE

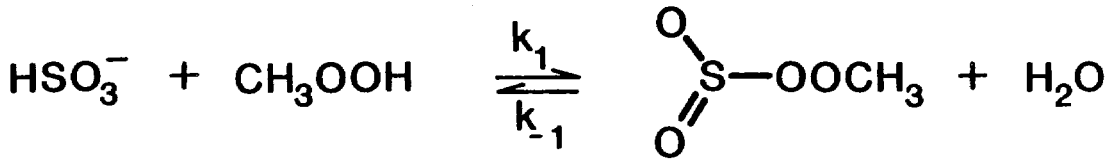

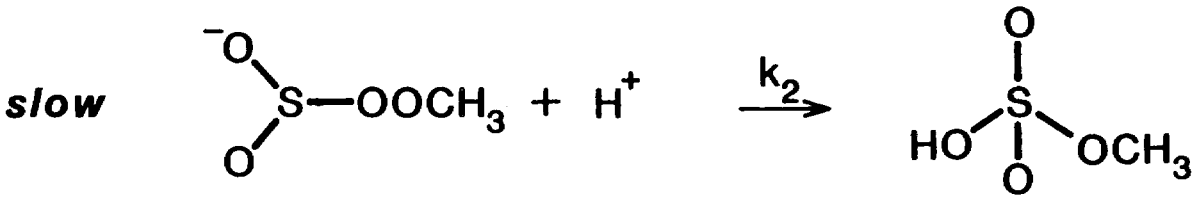

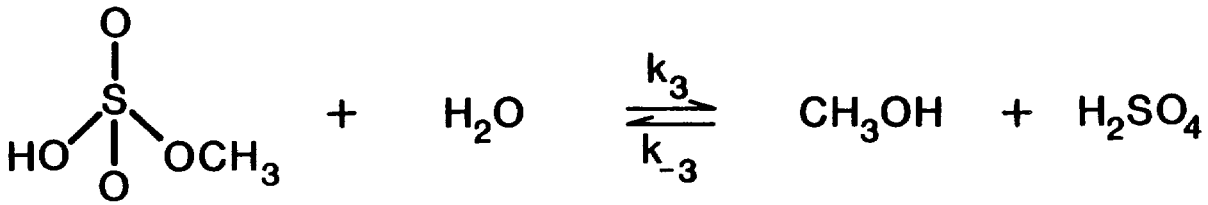

$K_3 = 0.11$ $k_3 = 7\times10^{-3}\ M^{-1}\ s^{-1}$

PEROXYACETIC ACID

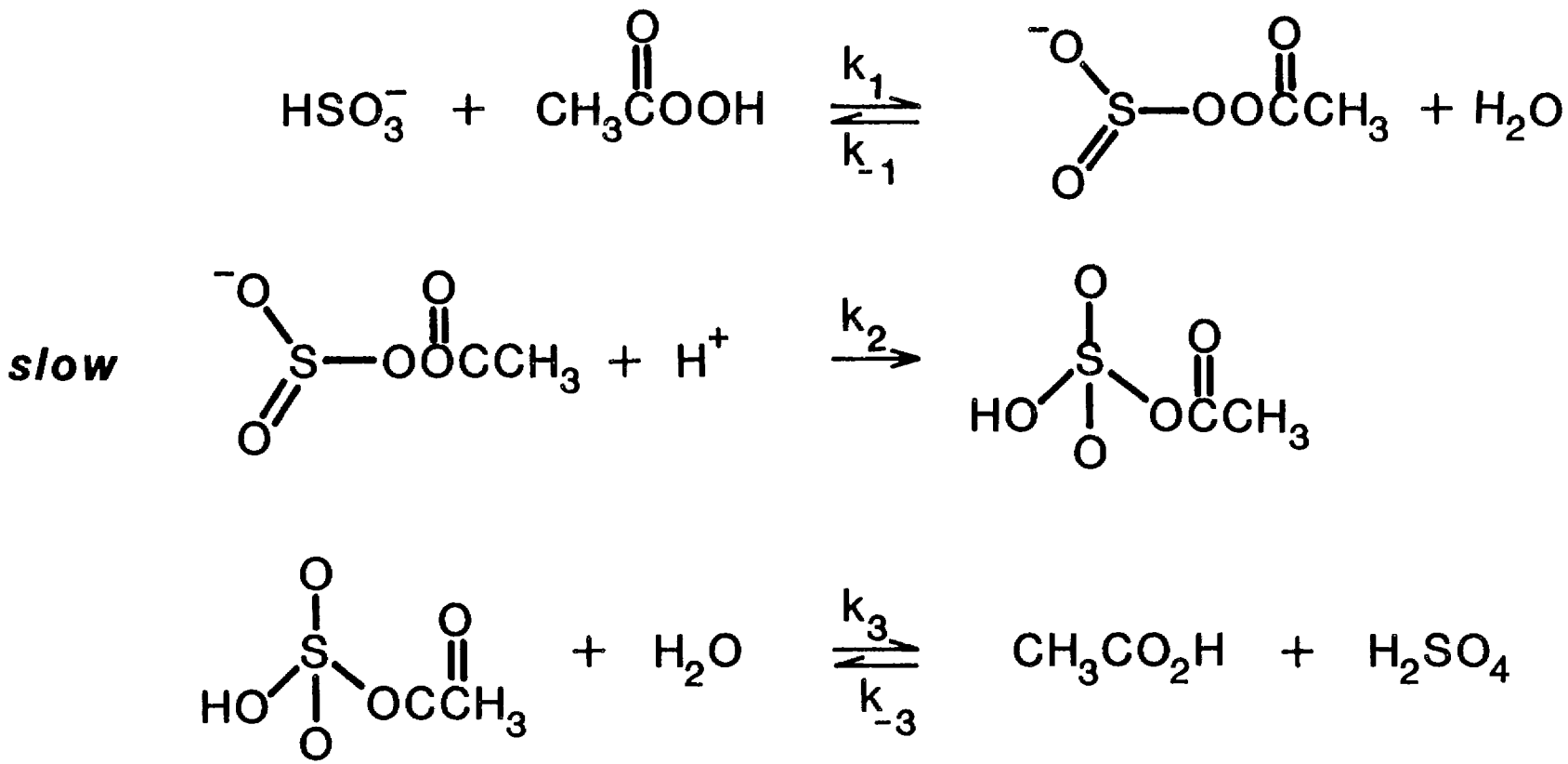

$$\nu = k[H^+][ROOH][HSO_3^-]$$

R	$k = k_2 k_1 / k_{-1}$ $(M^{-2} s^{-1})$*	K_{1t} $(M\ atm^{-1})$†
H—	7.2×10^7	7.4×10^4
CH_3—	1.7×10^7	2.2×10^2
$CH_3C(=O)$—	3.5×10^7	4.7×10^2

*Lind et al. (1987) 18 °C

†Lind & Kok (1986) 25 °C

S(IV) AND O_3

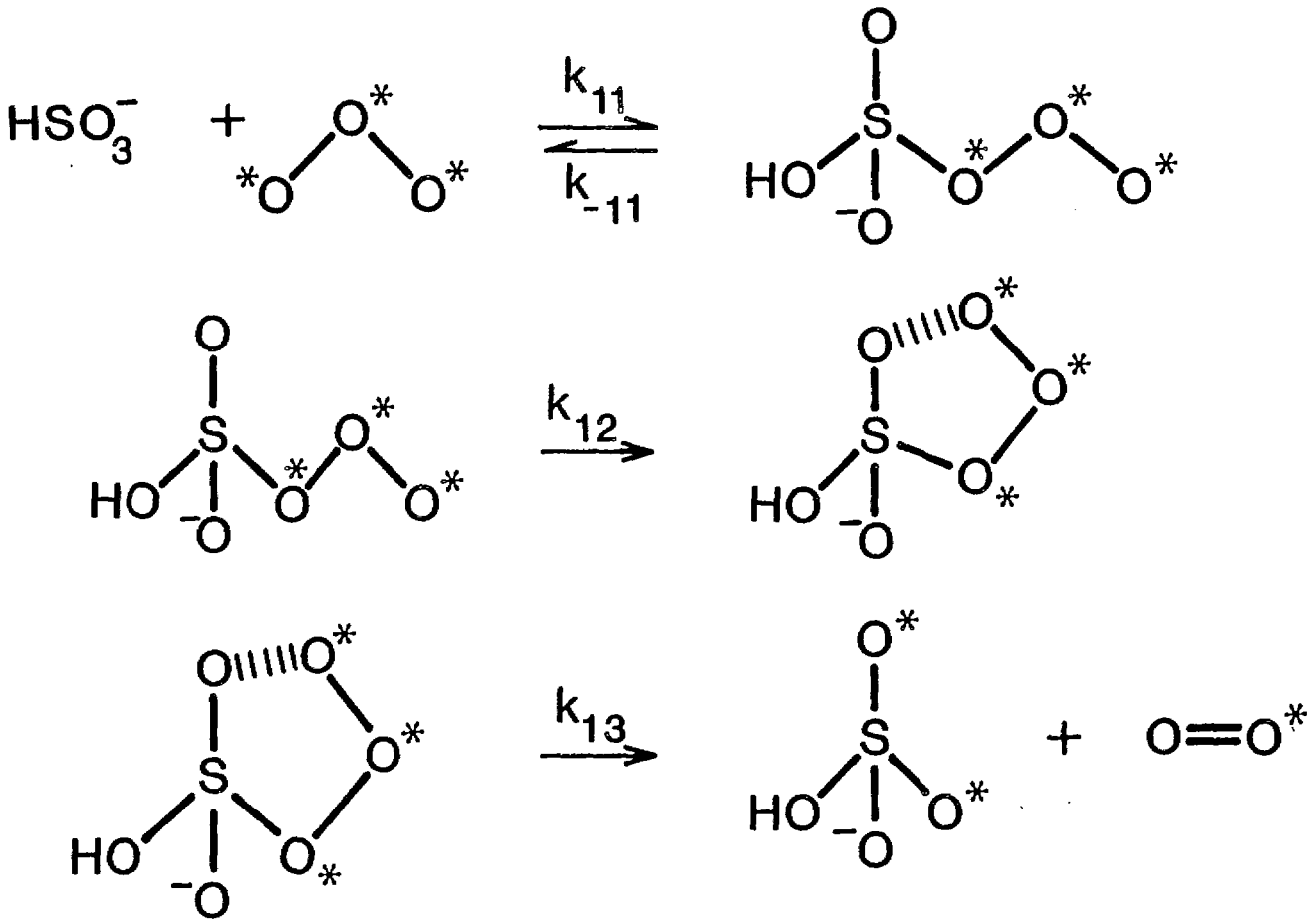

OXIDATION OF HONO BY H_2O_2

$$HNO_2 \underset{}{\overset{K_a}{\rightleftharpoons}} H^+ + NO_2^- \qquad pK_a = 3.15$$

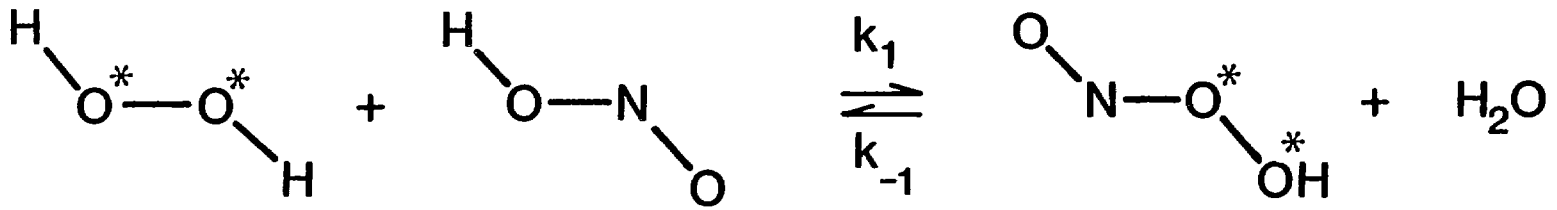

$$H^+ + \text{[peroxynitrous acid]} \xrightarrow{k_2} \text{[nitrate ion]} + 2H^+$$

$$\nu = \frac{k_2 k_1}{k_{-1}} [H^+][HNO_2][H_2O_2]$$

$$\frac{k_2 k_1}{k_{-1}} = 6.3 \times 10^3 M^{-2} s^{-1} \text{ (Lee \& Lind, 1986)}$$

Fe(III)-CATALYZED AUTOXIDATION OF S(IV)

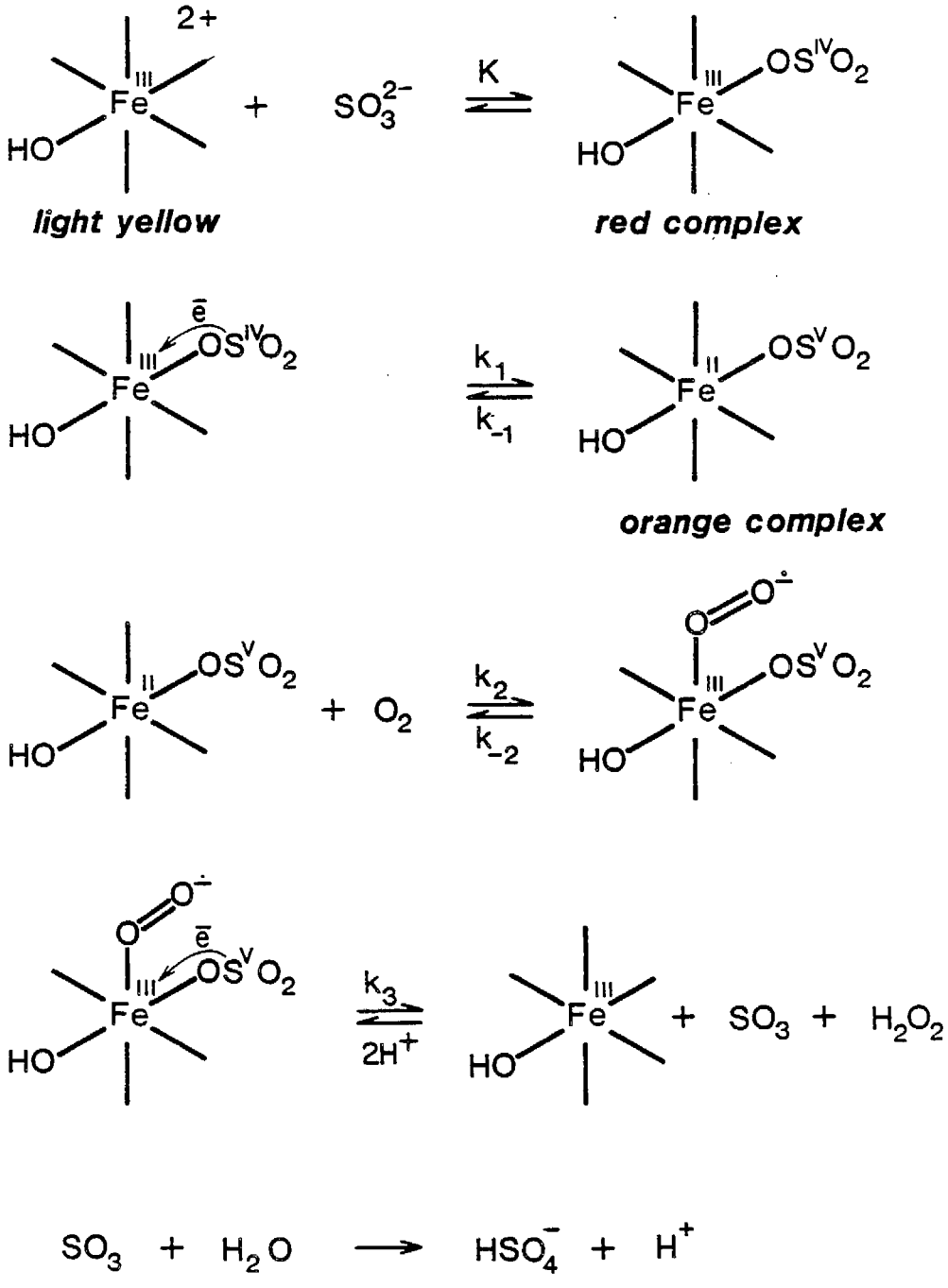

$$SO_3 + H_2O \longrightarrow HSO_4^- + H^+$$